2018 22nd International Conference on System Theory, Control and Computing (ICSTCC)

A resonant speed controller for injection of a sinusoidal speed excitation in frequency response analysis of variable speed pump drives

David Graurock
Research and Development
Wilo SE
Dortmund, Germany
david.graurock@wilo.com

Benedikt Meier
Research and Development
Wilo SE
Dortmund, Germany
benedikt.meier@wilo.com

Martin Oettmeier
Research and Development
Wilo SE
Dortmund, Germany
martin.oettmeier@wilo.com

Jens O. Fiedler
Research and Development
Wilo SE
Dortmund, Germany
jens.fiedler@wilo.com

Torsten Bertram
Institute of Control Theory and Systems Engineering
TU Dortmund University
Dortmund, Germany
torsten.bertram@tu-dortmund.de

***Abstract*—In this paper an approach for adapting a speed controller in order to perform a superposition of the speed of a circulating pump with a sinusoidal excitation is presented. In various applications the injection of a sinusoidal signal can be used for frequency response analysis. In this case the speed control of a circulating pump is adapted in order to perform a speed excitation which can be used for the identification of the pipeline network the pump is embedded in. As the original speed control was implemented with a PI-controller in order to control the operating point of the pump, the control is adapted by adding a resonant controller in parallel to the PI-controller in order to maintain a transfer function similar to the original one while providing an improved behaviour regarding the injection of the speed excitation.**

***Index Terms*—Control design, electric machines**

I. Introduction

THE injection of a sinusoidal signal is a typical approach in order to perform a frequency response measurement of a system at certain frequencies [1]. Regarding pump applications the injection of a sinusoidal speed variation can be used in order to investigate the dynamic behaviour of pumps [2]. In this case the speed of a circulating pump shall be superimposed with a sinusoidal speed excitation which can be used for identification purposes. Furthermore, the application of the presented approach is not limited to the injection of signals, but may be used to suppress an undesired frequency component such as a harmonic as well. The aim of the presented approach is to adapt the original speed controller in a way that the original design rule of the controller maintains its validity while the adaption provides an improved behaviour regarding the injection of the speed excitation.

The desired value of the speed of the considered pump can be set to a constant value or provided by a hydraulic controller in order to reach a certain hydraulic operating point such as a certain differential pressure. However, since the applications for which the pump might be used vary, the configuration and hence the hydraulic resistance and the time constants of the pipeline network the pump will be embedded in are not known in advance. Therefore, the hydraulic control is designed to be slowly in order to be compatible to pipeline networks with both slow and fast time constants.

Considering the relationship between pressure and volume flow [3] it can be seen that the structure coincides with the relationship between voltage and current in an electrical circuit that comprises a resistor and an inductance. Therefore, the hydraulic circuit can be represented analogously to an electrical circuit as depicted in Fig. 1 where Q represents the volume flow which depends on the hydraulic resistance R_{h} and the hydraulic inductance L_{h} of the pipeline network and the differential pressure p_{P} generated by the pump. Based on this representation a frequency response analysis can be performed. A sinusoidal speed excitation can be injected in order to cause variations of the differential pressure and as a result variations of the volume flow. Then, from the variation of the hydraulic quantities at the excitation frequency which is chosen to be $\omega_{\mathrm{H}} = 32.7\,\mathrm{rad/s}$ the pipeline network can be identified and the hydraulic control can be adapted to it.

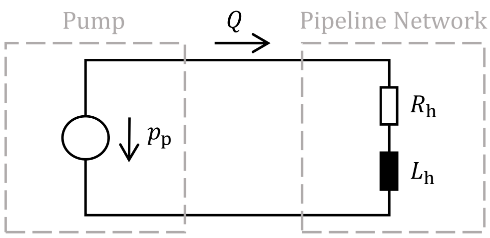

Fig. 1. Representation of the hydraulic circuit

In this case the initial speed controller was realised as a PI-controller and parametrised based on the symmetrical optimum approach as it is the typical approach for speed control loops with a subordinate current control loop [4]. As the speed controller was designed for control of the operating point not considering the injection of a sinusoidal speed excitation, the controller is not able to inject the signal at the desired frequency with the desired amplitude. Furthermore, at the desired frequency the amplitude of the speed modulation exhibits a behaviour which is dependent on the operating point of the pump. Therefore, the controller is adapted by adding a resonant controller in parallel to the PI-controller in order to perform the sinusoidal speed variation at the desired frequency while achieving a transfer function similar to the original one. This way, the desired behaviour of the speed controller can be maintained at frequencies other than the excitation frequency.

Furthermore, the speed controller incorporates safety functions which for example decrease the speed of the pump in case the maximum allowed power is exceeded in order to avoid damaging the drive of the pump. As these safety functions counteract the injection of the speed modulation, approaches are developed in order to be able to perform the speed modulation in the whole operating range.

II. Speed control

A. Initial design of the speed control

The speed controller initially used is realised by a PI-controller where the proportional part provides a fast dynamic behaviour and the integral part avoids steady state errors. A scheme of the closed loop speed control is shown in Fig. 2.

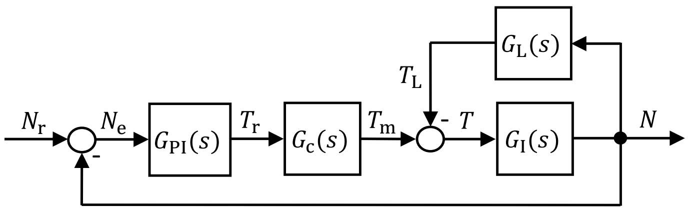

Fig. 2. Scheme of the closed loop speed control

The error N_e is calculated based on the reference speed N_r and the actual speed N of the pump. Depending on the error N_e the speed controller with the transfer function

$$G_\mathrm{PI}(s) = K_\mathrm{P} + K_\mathrm{I}\, s^{-1} \tag{1}$$

and the proportional gain K_P and the integral gain K_I generates the reference torque T_r. As the pump is driven by a permanent magnet synchronous machine, a subordinate current control loop $G_\mathrm{c}(s)$ is used for providing the stator currents which are necessary in order to generate the reference torque. The torque, actually generated by the drive, is denoted by T_m. The current control loop is approximated by a first order system with the time constant T_c:

$$G_\mathrm{c}(s) = \frac{1}{1 + s\, T_\mathrm{c}}. \tag{2}$$

The torque T_m is superimposed with a load torque T_L which is generated due to friction and the hydraulic load due to the transportation of the fluid by the pump. The relation between load torque and the speed of the pump is described by $G_\mathrm{L}(s)$. The speed N of the pump changes depending on the resulting torque T and the transfer function $G_\mathrm{I}(s)$:

$$G_\mathrm{I}(s) = \frac{1}{s\, I}. \tag{3}$$

The variable I incorporates the inertia of the motor shaft, the impeller of the pump and a conversion factor in order obtain the speed N instead of the angular frequency as output.

The speed controller is parametrised using the symmetrical optimum as it is the typical approach for speed control loops with a subordinate current control loop [4]. As the load torque T_L depends on the configuration of the pipeline network which can change with time for example by changes of valve positions, T_L is considered a disturbance and neglected for the design of the speed controller. The parameters of the speed controller are calculated as follows:

$$K_\mathrm{P} = \frac{I}{a\, T_\mathrm{c}}, \tag{4}$$

$$K_\mathrm{I} = \frac{K_\mathrm{P}}{a^2\, T_\mathrm{c}}. \tag{5}$$

The parameter a needs to be chosen. A low value of a leads to a fast compensation of disturbances and a fast dynamic behaviour at changes of the set point, but reduces the phase margin of the open loop system and causes an overshooting of the closed loop control at set point changes. On the other side a high value of a avoids the overshooting at the cost of a slower dynamic behaviour. Therefore, $a = 2$ is chosen since this value is recommended in order to achieve a compromise between dynamic behaviour and overshooting [4].

Although the parametrisation of the speed control was performed based on continuous transfer functions, the actual implementation is done in the time discrete domain. Still, the parametrisation based on continuous transfer functions can be considered valid since the mechanical time constants are much higher compared to the sample rate of the speed controller.

B. Influence of the operating point on the speed control

The influence of the load torque T_L was not considered during the design of the PI-controller. However, for the injection of a sinusoidal speed variation at the respective operating point the load torque needs to be considered in order to evaluate the impact of the operating point on the injected speed modulation.

The load torque T_L is modelled by a combination of friction terms and the hydraulic torque model according to [3] which represents the torque due to the hydraulic operating point:

$$T_\mathrm{L} = a_\mathrm{t}\, N\, Q - b_\mathrm{t}\, Q^2 - c_\mathrm{t}\, \frac{Q^3}{N} + \nu_\mathrm{i}\, N^2 + \nu_\mathrm{v}\, N + \nu_\mathrm{c}. \tag{6}$$

Hereby, a_t, b_t and c_t are parameters which depend on the geometry of the respective pump. The parameters ν_c, ν_v and ν_i are the coefficients of the coulomb friction, viscous friction and the friction between impeller and fluid, respectively.

Since the aim is to inject a sinusoidal speed variation at the current operating point, a linearisation of equation (6) can be performed. The change $T_\mathrm{L,1}$ of the load torque depending on the change Q_1 of the volume flow and the change N_1 of the speed is derived by linearisation of equation (6) for the respective operating point:

$$T_{\text{L},1} = \left(a_\text{t}\, Q_0 + c_\text{t}\, \frac{Q_0^3}{N_0^2} + 2\, \nu_\text{i}\, N_0 + \nu_\text{v} \right) N_1 + \\ + \left(a_\text{t}\, N_0 - 2\, b_\text{t}\, Q_0 - 3\, c_\text{t}\, \frac{Q_0^2}{N_0} \right) Q_1. \quad (7)$$

The variables Q_0 and N_0 represent the value of the volume flow and speed at which the linearisation is performed.

In order to eliminate Q_1 as an input quantity the relationship between Q_1 and N_1 is derived. The differential pressure p_P generated by the pump can by modelled as described by [5]:

$$p_\text{P} = a_\text{h}\, N^2 - b_\text{h}\, N\, Q - c_\text{h}\, Q^2. \quad (8)$$

The parameters a_h, b_h and c_h depend on the respective pump. The derivative of the volume flow with respect to the time t can be modelled as described by [3]:

$$\frac{\text{d}Q}{\text{d}t} = \frac{p_\text{P} - d_\text{h}\, Q^2}{L_\text{h}}. \quad (9)$$

The parameters L_h and d_h represent the hydraulic inductance and the hydraulic resistance of the pipeline network, respectively. Linearising equation (9) and applying the Laplace transform leads to the transfer function $G_{\text{p,Q}}(s)$ which represents the change Q_1 of the volume flow due to a change p_1 of the differential pressure provided by the pump:

$$G_{\text{p,Q}}(s) = \frac{Q_1(s)}{p_1(s)} = \frac{1}{s\, L_\text{h} + 2\, d_\text{h}\, Q_0}. \quad (10)$$

In case equation (8) is linearised for the operating point which is defined by the volume flow Q_0 and speed N_0 and combined with equation (10), the relationship between the change Q_1 of the volume flow and the change N_1 of the speed can be represented as shown in Fig. 3.

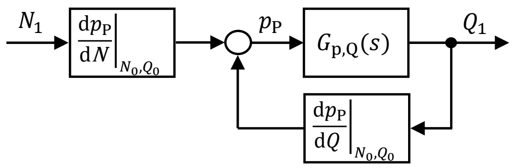

Fig. 3. Linearised transfer function between change of volume flow and speed

By combination of equation (7) and the volume flow model according to Fig. 3 the transfer function $G_\text{L}(s)$ between changes of the load torque and changes of the speed can be calculated for the respective operating point. Thus, the closed loop speed control loop shown in fig. 2 can be modelled with the influence of the load torque, but it has to be considered that due to the performed linearisation the model is only valid for small changes at the respective operating point.

The amplitude response of the closed loop speed control can be seen in Fig. 4. The amplitude response is shown for a load torque T_L = $0\,\text{Nm}$ since the load torque was neglected for the parametrisation of the PI-controller in section II-A. Furthermore, the amplitude response is shown with consideration of the load torque for two different speeds with two different volume flows, respectively. The first speed is $N_{0,1}$ = $830\,\text{rpm}$ and the volume flows are $Q_{0,1}$ = $0\,\text{m}^3/\text{h}$ and $Q_{0,2}$ = $20.7\,\text{m}^3/\text{h}$. The second speed is $N_{0,2}$ = $2010\,\text{rpm}$ and the volume flows are $Q_{0,1}$ = $0\,\text{m}^3/\text{h}$ and $Q_{0,2}$ = $50.3\,\text{m}^3/\text{h}$.

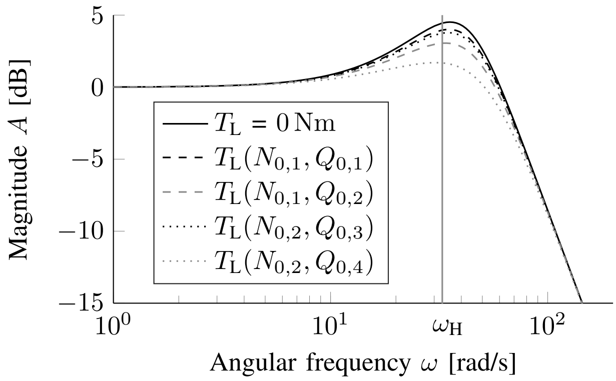

Fig. 4. Influence of the operating point of the pump on the amplitude response of the closed loop speed control

As can be seen for low and high frequencies the impact of the operating point on the amplitude response is low and thus neglecting the load torque for the parametrisation of the PI-controller only has a minor impact at these frequencies. Furthermore, at low frequencies the amplification A is close to A = $0\,\text{dB}$ and thus the PI-controller would suffice for the injection of the speed excitation. However, a desired injection frequency for the speed variation is ω_H = $32.7\,\text{rad/s}$ where the amplification differs from the value A = $0\,\text{dB}$ which is necessary in order to inject the speed variation with the desired amplitude. Furthermore, the amplification shows a dependence on the operating point at this frequency.

C. Adapted speed control

The speed controller should possess a high gain at the excitation frequency in order to be able to achieve a magnitude of the closed loop control which is close to A = $0\,\text{dB}$. Therefore, a resonant controller is used as it provides the advantage to possess a high gain at a certain frequency which in this case is the excitation frequency ω_H = $32.7\,\text{rad/s}$. Furthermore, it possesses a low gain at frequencies which are not close to the excitation frequency. In contrast to [6] where a resonant controller is used in series to a PI-controller in order to suppress harmonics, the approach in this paper is to use a resonant controller in parallel to the PI-controller combining them to a PIR-controller. Due to this approach the resonant controller is dominant at frequencies close to the excitation frequency because of its high gain in this region. At other frequencies the PI-controller is dominant due to the low gain of the resonant-controller at these frequencies. This way the behaviour of the original speed controller can be maintained at most frequencies and interference between the aim to reach the speed which is required for the hydraulic operating point and the aim to perform a superposition with the speed excitation can be minimised.

The transfer function $G_R(s)$ of a resonant controller is [7]:

$$G_R(s) = K_R \, \frac{s}{s^2 + \omega_H^2}. \tag{11}$$

The gain of the resonant controller can be influenced by the variable K_R. The angular frequency ω_H is the resonant frequency at which the controller reaches its highest amplification. As can be seen, the ideal resonant controller would even provide an infinite gain at the excitation frequency ω_H.

In order to perform a discrete implementation of the resonant controller the discretisation approach according to [7] is used. Therefore, the discrete transfer function $G_R(z)$ of the resonant controller is:

$$G_R(z) = K_R \, \frac{z - 1}{z^2 + (\omega_H^2 \, T_S^2 - 2) \; z + 1}. \tag{12}$$

A comparison of the frequency response of the discrete PI-controller and the discrete PIR-controller is shown in Fig. 5.

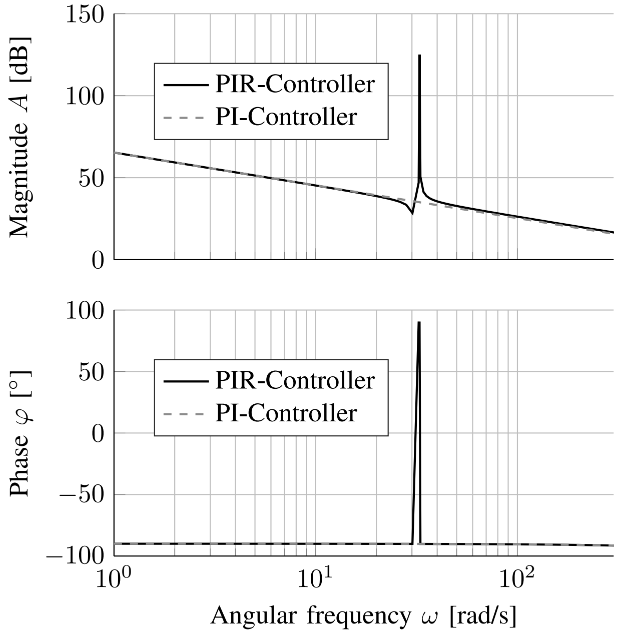

Fig. 5. Bode plot of discrete PI-controller and discrete PIR-controller

In contrast to the continuous ideal resonant controller the discrete implementation used for the PIR-controller does not provide an infinite gain at the excitation frequency $\omega_H = 32.7\,\mathrm{rad/s}$, but it still provides a high gain of $A = 125\,\mathrm{dB}$ at this frequency. Despite the different amplifications of PIR-controller and PI-controller close to the excitation frequency the PIR-controller provides a gain similar to the gain of the PI-controller at frequencies which are not close to the excitation frequency. Considering the phase shift the same behaviour is shown. Close to the excitation frequency the phase shift of the PIR-controller deviates from the phase shift of the PI-controller, but at other frequencies both controllers possess a similar phase shift.

III. Comparison of PI- and PIR-Controller

A. *Experimental setup*

The experimental setup which was used in order to validate the designed speed control is depicted in Fig. 6. The testbench is equipped with a volume flow and a pressure sensor in order to determine the hydraulic operating point of the pump. Furthermore, the testbench possesses a valve in order to vary the hydraulic resistance of the pipeline network and hence the volume flow. Since no sensor in order to measure the rotor position of the motor is available, the rotor angle of the motor is determined using a Back-EMF based approach [8]. Then, based on the rotor angle the speed of the motor is determined using a phase locked loop [9].

Fig. 6. Experimental setup with pipeline network and pump

B. *Experimental Results*

A measurement is performed with a DC part N_0 of the speed of $N_0 = 830\,\mathrm{rpm}$, $N_0 = 1340\,\mathrm{rpm}$ and $N_0 = 2010\,\mathrm{rpm}$ for the PI-controller and PIR-controller, respectively, in order to evaluate the performance of the controllers regarding the injection of the speed excitation. For each speed N_0 the measurement is performed at different hydraulic operating points by varying the volume flow. Starting with a volume flow of $Q = 0\,\mathrm{m^3/h}$ due to a closed valve, the valve is opened in certain steps in order to increase the volume flow until the valve is opened completely. Then, at each operating point the amplitude N_1 of the speed excitation is extracted based on the determined speed by applying a discrete fourier transformation. The reference amplitude of the speed excitation is set to $N_{1,r} = 30\,\mathrm{rpm}$ and the angular frequency of the speed modulation is chosen to be $\omega_H = 32.7\,\mathrm{rad/s}$.

As can be seen in Fig. 7 the amplitude injected by the PI-controller shows a dependency on the operating point. In case the volume flow has a value of zero due to a closed valve, the amplitude injected by the PI-controller increases with a decreasing DC part N_0 of the speed. If the valve of the pipeline network is opened in order to increase the volume flow, the amplitude of the speed excitation decreases with the increasing volume flow. In general this influence of volume flow and speed coincides with the modelled influence of the load torque from section II-B. Still, the model shows deviations from the measurements. For example, the model predicts a higher amplitude than the desired one for $N_0 = 2010\,\mathrm{rpm}$ and $Q_0 = 50.3\,\mathrm{m^3/h}$ as can be seen in Fig. 4, but the measurement shows an amplitude below the desired one. This difference can be explained by inaccuracies of the closed loop speed control model.

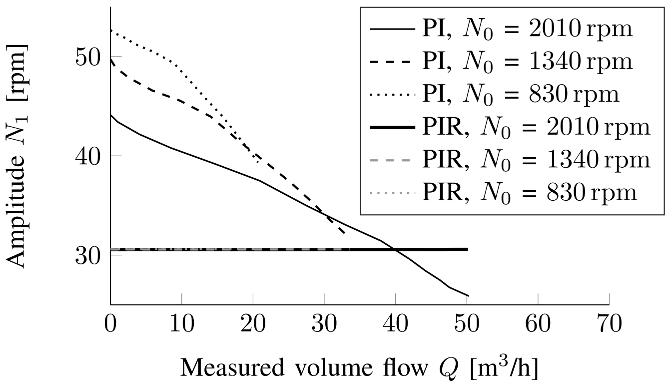

Fig. 7. Amplitude of speed excitation using PI-Controller and PIR-Controller

Due to the operating point dependency of the PI-controller the actual amplitude of the speed excitation possesses a value between $N_1 = 25.9\,\mathrm{rpm}$ and $N_1 = 52.6\,\mathrm{rpm}$ instead of the desired value $N_{1,\mathrm{r}} = 30\,\mathrm{rpm}$ which equals a maximum deviation of $75.3\,\%$.

In comparison to this behaviour the PIR-controller shows an improved behaviour. The injected amplitude has a maximum deviation of $2.0\,\%$ from the desired value which is in comparison to a maximum deviation of $75.3\,\%$ with the PI-controller a considerable reduction of the deviation. Furthermore, in contrast to the PI-controller the PIR-controller does neither exhibit a relevant dependence on the the volume flow nor DC part of the speed. Using the PIR-controller the achieved accuracy of the speed variation is considered sufficient since the deviation is small and the dependence on the hydraulic operating point is avoided.

IV. Speed modulation at limitations

One issue which has to be considered is the operation in limitation regions of the drive of the pump. The motor possesses safety functions which are supposed to ensure that limits such as the maximum allowed current are not exceeded. These limitations affect the speed of the pump as can seen in Fig. 8.

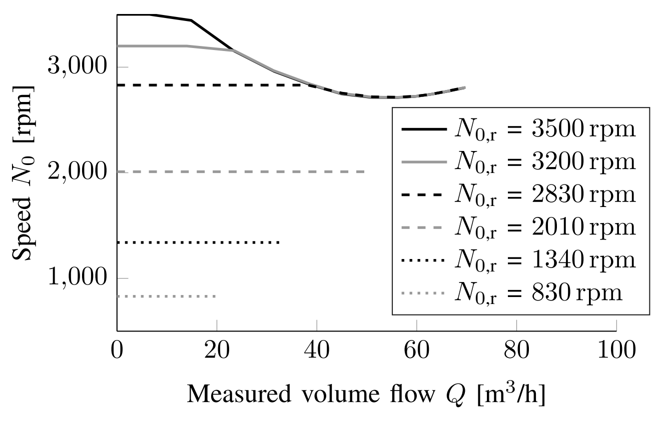

Fig. 8. Influence of drive limitations on the speed of the pump

At values of the DC part $N_{0,\mathrm{r}}$ of the reference speed which are within the low and middle speed region of the motor the actual DC part N_0 of the speed of the pump coincides with the desired value. At high speeds and high volume flows the allowed limits regarding current or power are reached. Therefore, safety functions become active which reduce the speed of the pump in order to avoid damaging the drive by exceeding the maximum allowed value of the current or power. As these safety functions affect the speed of the motor, the speed excitation is affected as well.

A. Current limitation

As explained in section II-A the generated torque T_m is provided by a current control loop. The current control is implemented as a field oriented control and the reference current $i_{q,\mathrm{r}}$ of the q-axis is calculated depending on the reference torque of the speed controller. In order to avoid exceeding the maximum allowed current the original current limitation incorporates the limitation of the reference value of the q-current to a fixed range. Furthermore, in case the reference current has reached its maximum value, the integral part of the original speed controller can only decrease its value in order to avoid a windup.

The speed excitation requires a variation of the torque and hence the value of the q-current. Thus, the desired speed excitation is not possible at currents close to the maximum allowed value as reference currents due to the speed excitation are clipped in case the maximum allowed current is exceeded. In order to avoid this issue the limitation of the PI-controller and the resonant controller are performed separately as shown in Fig. 9. The deviation N_e between the reference speed N_r and the actual speed N is calculated and forwarded to the PI-controller and the resonant controller. Both controllers generate the reference torques $T_{0,\mathrm{r}}$ and $T_{1,\mathrm{r}}$, respectively. Based on the reference torques the reference q-currents $i_{q0,\mathrm{r}}$ and $i_{q1,\mathrm{r}}$ are calculated. Then, both reference currents are limited and the final reference value $i_{q,\mathrm{l}}$ of the q-current is calculated based on the limited reference currents $i_{q0,\mathrm{l}}$ and $i_{q1,\mathrm{l}}$.

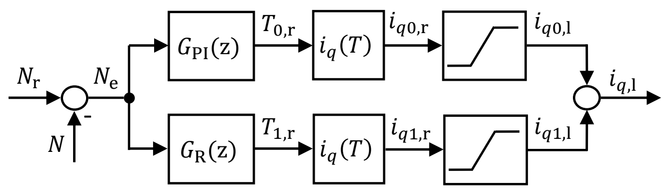

Fig. 9. Approach for separate current limitation of PI- and resonant controller

This approach provides the advantage that the reference current which is required for the desired operating point and generated by the PI-controller can be limited to the same value as before. The separate limitation of the resonant controller allows to limit the amplitude of the q-current which is generated by the resonant controller in order to provide the desired speed excitation. This way the maximum allowed reference value of the q-current can be exceeded for the speed variation. Since the speed variation with the frequency $\omega_\mathrm{H} = 32.7\,\mathrm{rad/s}$ and the corresponding variation of the q-current posses a sinusoidal shape, the maximum allowed q-current is only exceeded for a short time which is not an issue regarding thermal damage of the drive.

As can be seen in Fig. 8 in the limitation region there is a permanent deviation between reference speed and actual speed. This would not be an issue in case of an ideal resonant controller since it is not sensitive to the angular frequency $\omega = 0\,\mathrm{rad/s}$. In contrast to that, the non ideal discrete implementation reacts sensitive to DC offsets as can be seen in simulations. At normal operation this aspect is negligible because the PI-controller achieves zero steady state error, but during current limitation the permanent deviation between the DC part of the desired and the actual speed leads to an undesired oscillation of the output of the resonant controller. In order to avoid the influence of steady state errors on the resonant controller, the DC part of the input of the resonant controller is removed. This way the input of the resonant controller does not contain any DC part and the speed excitation can be performed in the current limitation region.

B. Power limitation

Another limitation which has to be considered is the power limitation. In case the maximum allowed power consumption of the pump is exceeded, a controller which reduces the reference speed becomes active in order to decrease the power consumption to the maximum value. Due to the adaption of the reference speed, the modulation of the speed and hence the power consumption is affected as well since the limitation controller tries to suppress the speed modulation in the limitation region.

In order to avoid interference of the power limitation with the speed modulation the average power consumption over the current modulation period is calculated. Then, instead of the current power consumption the average power consumption over the current modulation period is used for the power limitation. Since the purpose of the power limitation is to avoid exceeding the maximum power for a long time in order to avoid overheating of components, a short exceedance of the power limitation which is possible due to adapted approach is allowed.

This way the speed excitation can be performed even in limitation regions as can be seen in Fig. 10.

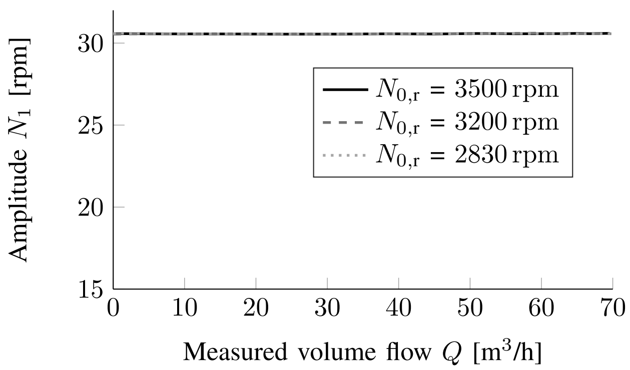

Fig. 10. Amplitude of speed modulation with adapted limitation approaches

V. Conclusion and Outlook

In this paper an approach for adapting a simple speed control in order to superimpose a speed variation was presented. The presented approach allowed to inject the desired speed excitation with a maximum deviation of $2.0\,\%$ from the desired amplitude which is a great improvement compared to a maximum deviation of $75.3\,\%$ using the original PI-controller based speed control. Furthermore, the adapted speed controller possesses a similar transfer function compared to the original speed controller which was designed for controlling the operating point. This provides the advantage that despite the adaption of the speed control a similar behaviour regarding the control of operating points can be achieved.

An issue which had to be considered was the injection of the speed excitation close to the power and current limits of the drive of the pump. As these safety functions mean to avoid damaging of the drive due to high temperatures, temporarily exceedances of the limits can be tolerated. This allowed to develop approaches in order to perform the speed excitation within limitation regions of the drive of the pump.

Further research should be dedicated to the applications allowed by the presented speed controller. As mentioned in section I, one aspect is the application for the identification of hydraulic networks. Since the parameters of the pipeline network could be identified based on the injected speed excitation and the corresponding change of the hydraulic quantities, an adaptive hydraulic controller might be developed in order to improve the quality of the hydraulic control of the pump.

References

[1] R. Isermann and M. Münchhof, *Identification of Dynamic Systems*. Berlin, Heidelberg: Springer Berlin Heidelberg, 2011.

[2] H. Tsukamoto, H. Yoneda, and K. Sagara, "The Response of a Centrifugal Pump to Fluctuating Rotational Speed," *Journal of Fluids Engineering*, vol. 117, no. 3, pp. 479–484, 1995.

[3] R. Isermann, *Mechatronische Systeme*, 2nd ed. Berlin, Heidelberg: Springer Berlin Heidelberg, 2008.

[4] D. Schröder, *Elektrische Antriebe - Regelung von Antriebssystemen*, 3rd ed. Berlin, Heidelberg: Springer-Verlag Berlin Heidelberg, 2009.

[5] C. S. Kallesøe, "Fault Detection and Isolation in Centrifugal Pumps," Ph.D. dissertation, Aalborg Universitet, 2005.

[6] M. Ruderman and T. Bertram, "Variable proportional-integral-resonant (PIR) control of actuators with harmonic disturbances," in *IEEE International Conference on Mechatronics*, 2013, pp. 847–852.

[7] S. A. Richter and R. W. de Doncker, "Digital proportional-resonant (PR) control with anti-windup applied to a voltage-source inverter," in *Proceedings of the 2011 14th European Conference on Power Electronics and Applications (EPE 2011)*, 2011, pp. 1–10.

[8] B. Meier, M. Oettmeier, J. O. Fiedler, and T. Bertram, "Geberlose Positionserkennung zur Regelung von permanentmagneterregten Synchronmaschinen," in *Fachtagung Mechatronik 2017*, 2017, pp. 209–214.

[9] M. Eskola, *Speed and position sensorless control of permanent magnet synchronous motors in matrix converter and voltage source converter applications*, ser. Publication / Tampere University of Technology. Tampere: Tampere University of Technology, 2006, vol. 639.